RESEARCH ARTICLE

Motoo Ukawa

Deep low-frequency earthquake swarm in the mid crust beneath Mount Fuji (Japan) in 2000 and 2001

Abstract Beneath Mount Fuji, the highest active volcano in Japan, deep low-frequency (DLF) earthquake activity has been monitored since the early 1980s. The DLF earthquakes occurred in the mid-crustal depth range, and burst-type activity lasting from several minutes to 30 min was detected 10 to 20 times in an ordinary year. The DLF earthquake activity increased sharply in the period from October 2000 to May 2001, showing swarm-like activity. The occurrence rate during the DLF earthquake swarm was approximately 20 times higher than the usual activity, and the wave energy released during the swarm period was twice as high as the total wave energy during the past 20 years. The DLF earthquakes in the period from 1987 to 2001 were relocated by estimating station corrections in order to reduce the effect of the change of seismic station distribution. The epicenters of most DLF earthquakes occurred in an elongated region with a long axis of about 5 km, whose center is located 2–3 km NE from the summit. A few percent of the DLF earthquakes, however, occurred around the summit area, significantly apart from the main epicenter region. The focal depths of well-located DLF events range from 10 to 20 km. During the high activity period in 2000 and 2001, most DLF events occurred within this main hypocenter area. The sharp increase of DLF earthquake activity at Mount Fuji started immediately after magma discharge and intrusion events in the Miyake-jima and Kozu-shima regions in July and August 2000. The tectonic and volcanic activity changes around the area suggest that the DLF earthquake swarm at Mount Fuji was triggered by the change of state of the deep magmatic system around Mount Fuji.

M. Ukawa (✉)
National Research Institute for Earth Science and Disaster Prevention,
Tennodai 3–1,
Tsukuba-shi, Ibaraki-ken 3005-0006, Japan
e-mail: ukawa@bosai.go.jp
Tel.: +81-29-858-1004
Fax: +81-29-851-5658

Introduction

Deep low-frequency (DLF) earthquakes have been reported in various volcanic regimes, such as volcanic areas of subduction zones (Ukawa and Ohtake 1987; Hasegawa and Yamamoto 1994; White 1996), hot spot volcanism in Hawaii (Koyanagi et al. 1987), and Long Valley caldera in the Basin and Range province (Hill 1996), indicating deep magmatic activity from the uppermost mantle to the mid crust. At Mount Fuji, the largest composite stratovolcano in Japan, DLF earthquake activity between 10 and 20 km was first reported in the early 1980s (Ukawa and Ohtake 1984), and since then the activity has been monitored by the National Research Institute for Earth Science and Disaster Prevention (NIED), Japan. In 2000 and 2001, the DLF earthquake activity at Mount Fuji abruptly increased to a level more than 20 times higher than the normal level of the previous 20 years.

The DLF earthquakes are an invaluable indicator of the state of activity of the deep portion of volcanoes. Although most DLF earthquakes have occurred independently of shallow volcanic activity, there have been some convincing cases of the close relationship between magma movements and the triggering of DLF earthquakes. For example, during the 2000 Pinatubo eruption, swarm-like DLF activity took place at a depth ranging from 30 to 40 km (White 1996), and at Iwate volcano DLF earthquakes increased during the shallow seismic activity that was induced by magma intrusion into the upper crust (Nakamichi et al. 2003).

Geologically the activity of Mount Fuji started about 100,000 years ago, and its activity is divided into two stages, Older Fuji (>11 ka) and Younger Fuji (<11 ka). The volcanic rocks of both stages are basalt with subordinate basaltic andesite. The total volume of all erupted products in the Younger Fuji period is estimated to be 47 km^3, 83% of which erupted in the early stage of Younger Fuji, from

11,000 to 8,000 years ago. For the most recent 3,200 years, the magma discharge rate is estimated to be 0.1 km^3 (DRE) per 100 years (Miyaji 1988).

Historically, 10 eruptions including three large eruptions have been recorded in written documents since the first eruption in 781 A.D. (Koyama 1998). The most recent eruption is the Hoei eruption in 1707 (VEI=5), about 300 years ago. In view of the geologic and historic activity of Younger Fuji period, it is apparent that Mount Fuji has a fairly high possibility of eruption over the long term. The sharp increase of the DLF earthquake activity, therefore, has prompted preparation for a future eruption, specifically the Hazard Map Project of Mount Fuji.

This study aims to evaluate temporal changes of DLF earthquakes at Mount Fuji based on long term seismic monitoring data which started in 1980, by focusing on the occurrence rate change and hypocenter locations. Chronologically the DLF earthquake swarm at Mount Fuji started immediately after volcanic activity in the area around Miyake-jima and Kozu-shima (Nakada et al. 2001; Sakai et al. 2001) in July and August 2000. This area is about 100 km south of Mount Fuji. Because of the chronological coincidence and because of the large intrusion volume of magma, 1 km^3, between Kozu-shima island and Miyake-jima (Nishimura et al. 2001), we will examine the possibility of DLF earthquake swarm triggering by dike intrusion.

The spectral structures of the DLF earthquakes at Mount Fuji exhibit a fairly wide variety. In this study, however, we will focus mainly on the hypocenter distributions and will describe the spectral variety in another report.

Seismic network and seismograms

In the early 1980s, the NIED constructed the Kanto-Tokai seismic network in central Japan to study the hypocenter areas in the wake of the Tokai and Kanto great earthquakes (Hamada et al. 1985). Because Mount Fuji is located at the center of this seismic network, the seismicity of Mount Fuji has been under investigation at the micro-earthquake level for this period, and the DLF earthquakes at Mount Fuji were first detected by this seismic network in 1983 (Ukawa and Ohtake 1984). However, the distance between the summit of Mount Fuji and the closest station (TR2) was more than 20 km within the Kanto-Tokai seismic network as shown in Fig. 1.

In the late 1980s, two seismic stations, SSN and SHJ were added to improve the detection level of DLF events at Mount Fuji (Fig. 1). In 1990, the NIED started the Mount Fuji volcanic research project to investigate the volcanic activity of Mount Fuji, and added four stations, FJN, FJY, FJS and FJH, during the period from 1990 to 1998 (Fig. 1). At these stations, three component seismometers and two component tiltmeters have been installed at the bottom of 200-m-deep boreholes.

In April 1995, seismic data processing targeting the Mount Fuji area was initiated by using the Fuji observation network. It comprised the four stations in the Mount Fuji area and seven stations from the Kanto-Tokai seismic network around Mount Fuji. In January 2000, the data processing system was improved, with several other stations within the Kanto-Tokai seismic network in the eastern side of Mount Fuji added in order to raise the detection level.

The NIED has routinely determined the hypocenters of earthquakes around the Mount Fuji area by using the Fuji observation network. In the course of data processing, deep low-frequency earthquakes have been identified. Figure 1 shows the hypocenter distribution of all events determined routinely during the period from April 1995 to December 2003. Here we observe a cluster of DLF earthquakes centered on the northeastern side of Mount Fuji at depths ranging mainly from 10 to 20 km. The hypocenters usually contain events with less reliable locations, because we wish to locate as many earthquakes as possible within the region to monitor temporal changes.

Seismograms of DLF earthquakes at Mount Fuji exhibit the following characteristics: (1) successive occurrence of events over a period of a few minutes to a few tens of minutes, (2) clear shear wave arrivals with amplitudes usually larger than P waves, (3) a predominant frequency range between 1 and 5 Hz, and (4) in some cases P and S arrivals exhibit hybrid spectral nature, that is, high frequency waves (>10 Hz) superposing on the predominant low-frequency waves (<5 Hz). These are common characteristics among DLF earthquakes in many areas (Ukawa and Obara 1994; Hasegawa and Yamamoto 1994).

Figure 2 shows typical example of DLF earthquake seismograms on November 11, 2000. The seismograms were recorded at the FJN station with borehole type short period seismographs (f0=1 Hz). The upper trace is the vertical component seismogram showing successive occurrences of DLF earthquakes for more than 3 min. The middle traces are three component seismograms for a part of the upper seismogram for 20-s intervals. A set of clear P and S arrivals is identified on the seismograms. In this case, both P and S phases have spectral peaks between 2 and 4 Hz as shown at the bottom. The low-frequency nature of the seismograms clearly contrasts with the spectra for ordinary local earthquakes of the same magnitude level, in which spectra between 10 and 20 Hz are usually predominant. The spectral difference makes it easy to distinguish the DLF earthquakes from ordinary earthquakes with higher frequency ranges.

Temporal change of the earthquake activity

The tendency for DLF earthquakes to occur in quick succession makes it difficult to record an accurate number of earthquakes with some threshold level, due to overlapping seismic codas, especially in the case of large events. For the purpose of evaluating the temporal variation of the activity, therefore, we count one continuous vibration composed of multiple DLF earthquakes as one event, measuring the duration time and maximum amplitude. For example, the DLF event shown in Fig. 2 is counted as one event.

Figure 3 shows the occurrence of DLF events from 1980 to the end of 2003. The height and width of each

Fig. 1 a Map showing station locations of the NIED and hypocenters determined routinely by the NIED during the period from April 1995 to December 2003. Small and large marks (+) indicate stations belonging to the Kanto-Tokai network and those belonging to the Fuji observation network, respectively. Three sub-regions named as Fuji, East Yamanashi and Hakone are indicated by rectangles with broken lines. The topographic contour interval is 500 m. **b** E–W vertical cross section of all hypocenters plotted in **a**. **c** N-S vertical cross section of all hypocenters plotted in **a**. *Black circles* indicate the DLF earthquakes
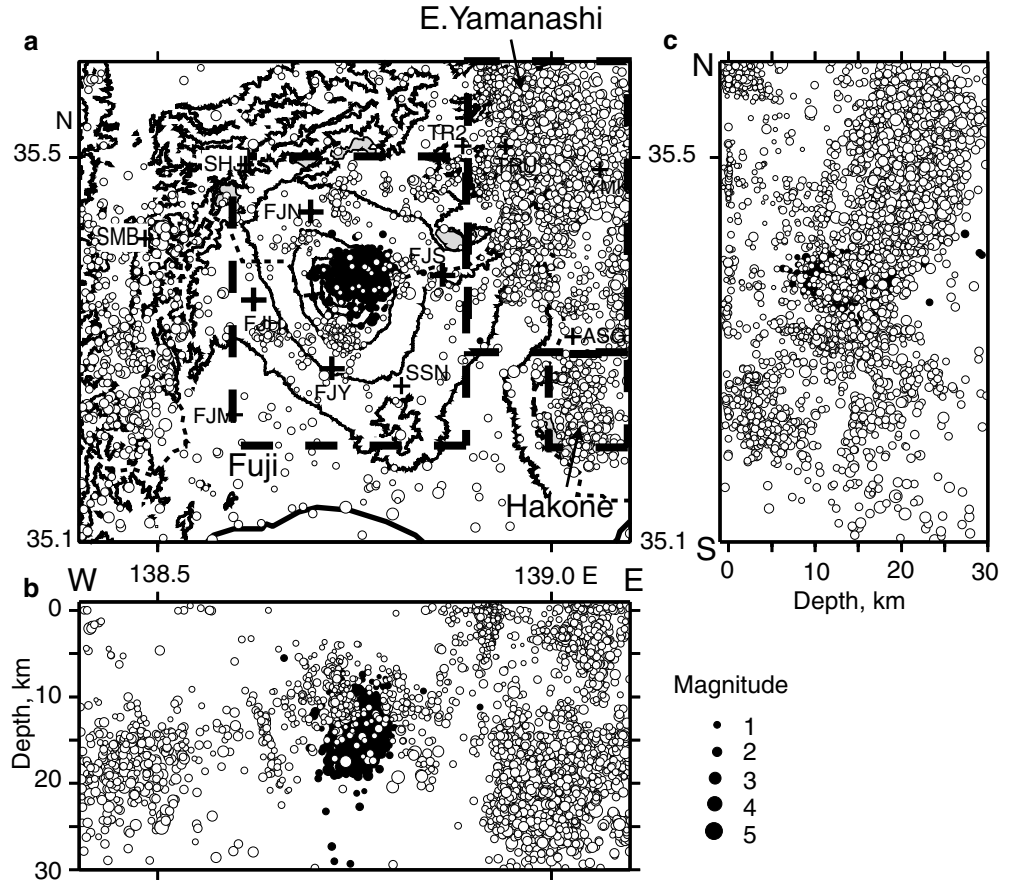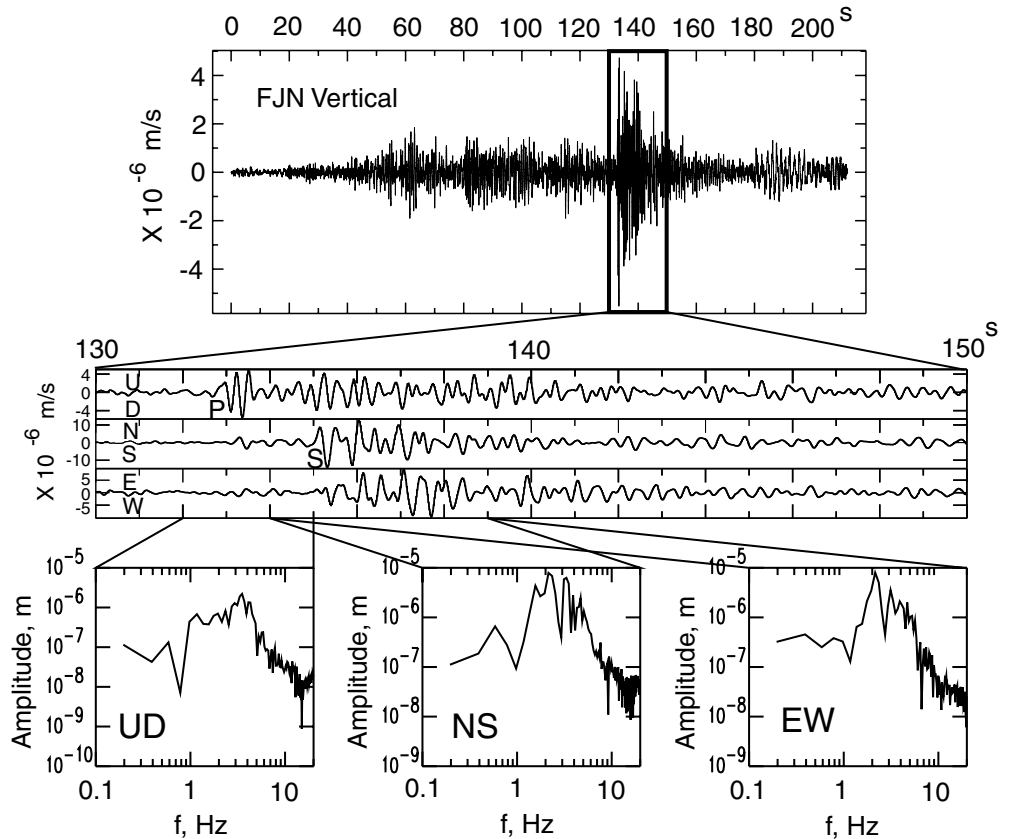
Fig. 2 (*Top*) Vertical component seismogram of a DLF earthquake on November 11, 2000, recorded at FJN station. (*Middle*) Three component seismograms at FJN for a 20 s interval of the seismogram shown above. (*Bottom*) Spectra of P wave on vertical component and those of *S* wave on horizontal components showing the predominant frequencies between 2 and 4 Hz
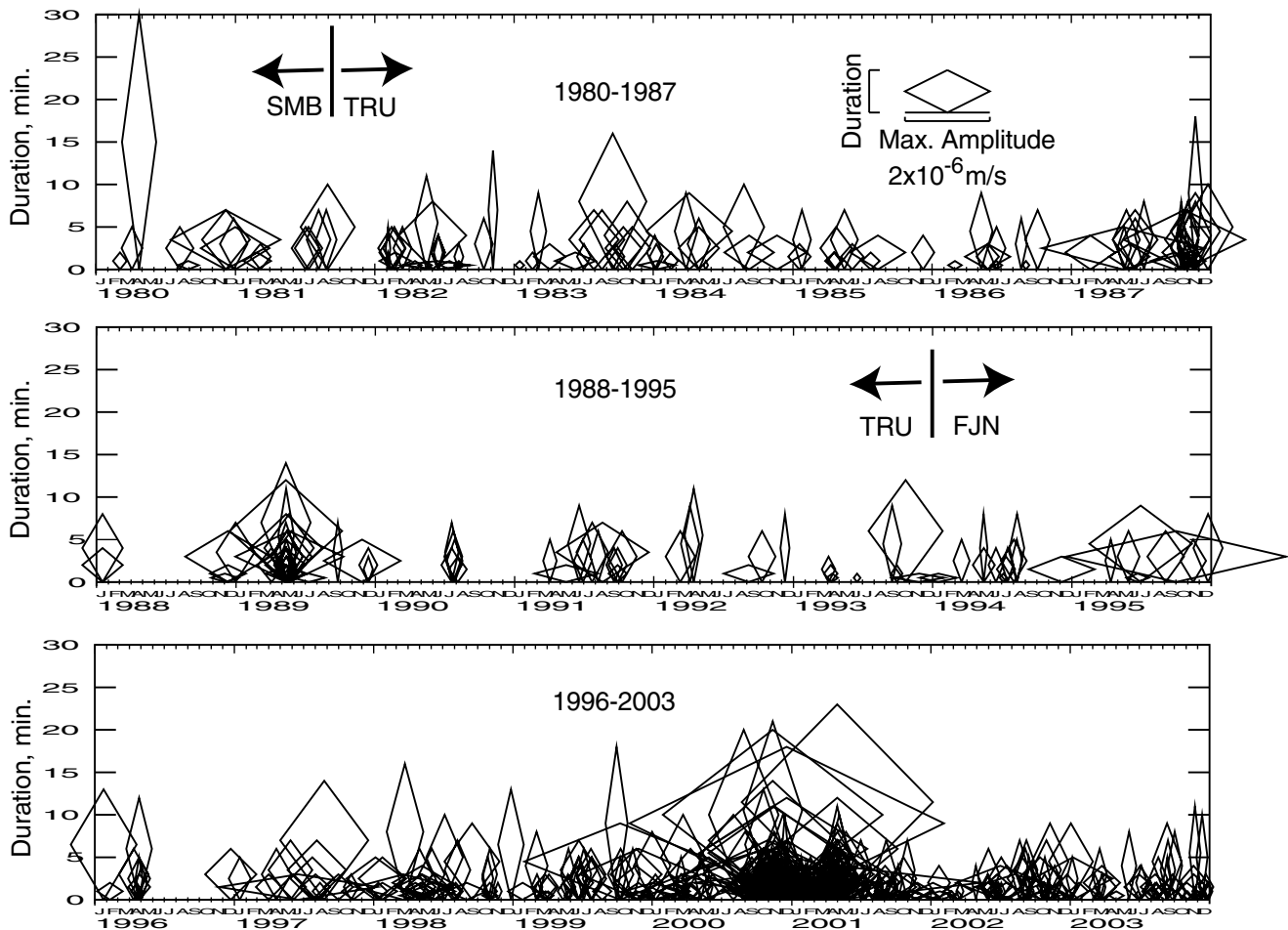
Fig. 3 A diamond diagram showing the activity of the DLF events at Mount Fuji. The height and width of each diamond represent the duration time and the maximum amplitude of each DLF event that is composed of successive DLF earthquakes. The duration time and the maximum amplitudes have been measured on the seismogram of the selected station indicated in the figure

diamond in Fig. 3 correspond to the duration time and the maximum amplitude of an event, as measured on the seismograms of selected stations (the SMB station from 1980 to August 1981, the TRU station from August 1980 to December 1993, and the FJN station from 1994 to 2003). The locations of stations are indicated in Fig. 1. In the diamond diagram, we also can plot events whose hypocenters were not determined. Because of the difficulty of locating DLF earthquakes, this diagram is useful in understanding temporal trends.

Before plotting the maximum amplitude, we examine amplitude station dependence. The epicenter distances from the principle DLF earthquake zone to SMB, TRU and FJN are 25, 23 and 10 km, respectively. The averaged amplitude ratios of SMB and FJN to TRU are 1.2 with the range from 0.3 to 3.3 for 119 events from 1982 to 1991, and 1.0 with the range from 0.5 to 2.1 for 12 events in 1994, respectively. The amplitude ratios are close to 1, although the scatter is large. No amplitude correction, therefore, was made for any of the three stations in the present plot.

If we assume the epicentral distances from the DLF earthquakes to the selected stations are similar, magnitudes of all the DLF events can be roughly estimated from the max-

imum amplitude data of one station plotted in Fig. 3. The estimated magnitudes range from 1.8 to–0.6 for the events in the 24 years recorded, indicating that all the DLF events are limited to the micro-earthquake level.

As onset and termination of DLF events are often unclear, it is difficult to measure their duration times accurately. Therefore, the duration times were measured by the minute on continuous monitoring records. The observed durations range up to 30 min, with most events shorter than 10 min. The total number of DLF events in this period is 711, 275 events of which occurred in the 20 years from 1980 to 1999 during which no significant earthquake swarm occurred. The average occurrence rate of DLF events is 14 per year, classified as background activity in an ordinary period. Some moderately high activity is recognizable even in the ordinary period, for example in the years 1987 and 1989.

In Fig. 3 the most noticeable feature is swarm-like activity in 2000 and 2001. In total, 286 events were identified during the 8 months from October 2000 to May 2001. The occurrence rate in this period is more than 20 times higher than normal. In order to objectively evaluate the temporal variation of the DLF earthquake activity, the cumulative number and cumulative wave energy are plotted in Fig. 4.
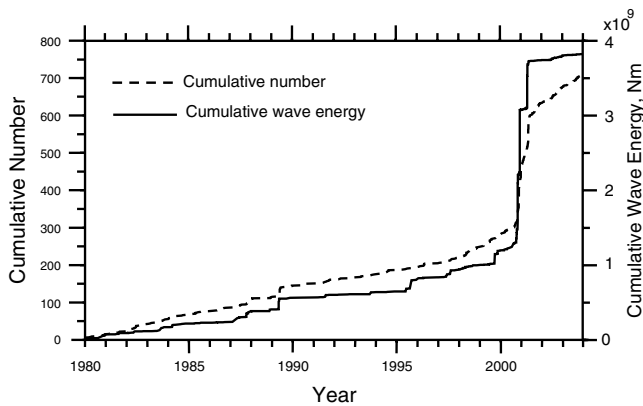
Fig. 4 Cumulative number of the DLF events (*dotted curve*) and cumulative wave energy (*solid line*) since 1980. Both are calculated from the same database as shown in Fig. 3

The increase rate of the cumulative number, or the slope of the curve, is almost constant before 1995, followed by a gradual increase before the DLF earthquake swarm. The reason for the gradual increase between 1995 and 2000 is due to the improvement of the seismic network around Mount Fuji and the new data processing system for Mount Fuji as described in the previous section. It is clear in Fig. 4 that the sharp increase in 2000 and 2001 is far larger than the artificial effect of the seismic network.

The wave energy for a DLF earthquake is estimated as follows: The average energy flux of a sinusoidal plane wave with an amplitude V and with a propagation velocity c is $(1/2)c\rho V^2$, where ρ is a density of the medium (Aki and Richards 2002). By taking into account a wave train of a DLF event with a maximum amplitude V_M at a hypocentral distance R, and with a duration time T_d, the total wave energy E_w propagating through a sphere of a radius R centered at the hypocenter is roughly calculated as $E_w=2k\pi\rho cT_dR^2V_M^2$. The parameter k in the equation of E_w is introduced to correct the effects of using the maximum amplitude, instead of the true wave train, to estimate the total wave energy, and is assumed to be 0.5 in this study. In the calculation of Ew we adopted following values, ρ=2,600 kg/m^3, c=3.5 km/s and R=20 km. Although this calculation of wave energy is simplified and an estimate, it provides a means to express source magnitudes, which are different from the cumulative number.

The total wave energy during the DLF earthquake swarm period in 2000 and 2001 is about twice as much as the total value during the past 20 years, indicating that relatively large events took place during the swarm period. On the cumulative wave energy curve, no significant increase of the wave energy emission by the DLF earthquakes was identified before the swarm. This curve also indicates that the emission rate of the wave energy returned to normal levels after the cessation of the DLF earthquake swarm in May 2001. Both of the cumulative curves in Fig. 4 clearly show a significant increase in the DLF earthquake in 2000 and 2001.
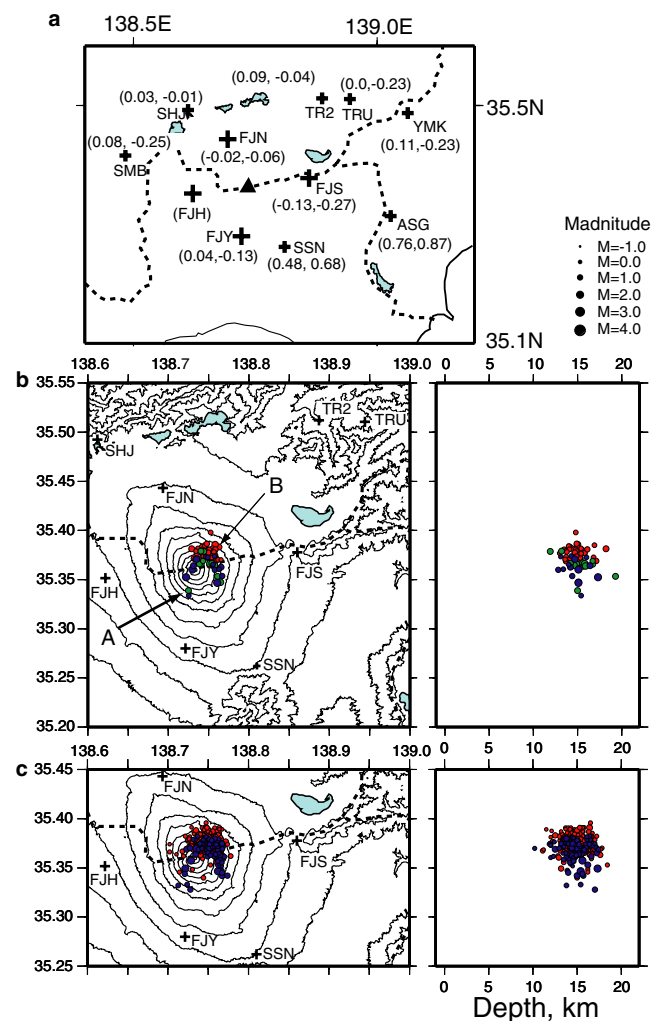

Fig. 5 a Map showing the locations of stations used for relocation of the DLF earthquakes. The *numbers in the parentheses* are station corrections (O–C) for P and S arrivals. The stations with a small mark (+) were constructed in the 1980s, and those with a large mark (+) in the 1990s. **b** Hypocentral distribution of the selected events with highest reliability of arrival times since 1987. The hypocenters are determined simultaneously with the station corrections described in the top figure. Hypocenters in three chronological intervals are indicated in different colors; *green* for 1987–March 1995; *blue* for April 1995–July 2000; and *red* for August 2000– May 2001. **c** Hypocentral distribution of the DLF events located by using the station corrections. The arrival times are picked up in this study, and the events with better pick-up times are selected. The colors are the same periods as in **b**. *Dashed lines* indicate boundaries of prefectures. The topographic contour interval in **b** and **c** is 300 m

Hypocenters

Station corrections for hypocenter calculation

The seismic network has been improved around Mount Fuji since 1980 as shown in Fig. 5a, and the seismic data around Mount Fuji have been processed independently from other areas by using selected stations close to Mount Fuji since 1995. The change of condition affects not only the detection level of the DLF earthquakes but also hypocenter locations.

In this study we will examine hypocenter locations by relocating them and applying station corrections to reduce the effect of changing station distributions with time.

We selected 10 stations within 30 km of the summit as the target for the relocation period from 1987 to 2001. The number of stations, however, changed during this time. From 1987 to 1995, the number of stations was seven, and the closest station was SSN, located 15 km from the summit. From 1995 to 1998, four stations (FJN, FJY, FJS and FJH) in the foothill region of Mount Fuji were added, but due to timing clock problems at the FJH station, FJH was not used in this relocation. Since 1998, 10 stations in Fig. 5a have been available.

In order to obtain reliable hypocenters, the arrival times of DLF earthquakes obtained by the Mount Fuji seismic network from April 1995 to May 2001 are reexamined in this study, and 369 events with good readings among 859 events are selected in the process. Among the 369 events, a further 57 events with better readings are selected for station correction estimation. In addition to this dataset, 13 DLF earthquakes with clear arrivals, which are also reexamined in this study, are selected for the period from 1987 to 1994.

In the first step, station corrections for 10 stations are estimated for the hypocenters of 70 events with high quality arrival times. The standard velocity structure is a horizontally layered structure comprising five layers as indicated in Table 1, which is constructed on the basis of the seismic velocity structure for the routine hypocenter determination within the Kanto-Tokai seismic network (Ukawa et al. 1984). The crustal thickness is taken as 29 km for this model. The seismic velocity above sea level is assumed to be same as the first layer in Table 1.

The station corrections and hypocenters are determined simultaneously by applying the same method as Ukawa et al. (1988), which is based on Crosson (1978). In the calculation, the P station correction for the TRU station is fixed as 0 because of the non-uniqueness problem between station corrections and origin times. The resulting station corrections range from -0.13 s to 0.76 s for P arrivals and from -0.27 s to 0.87 s for S arrivals as shown in Fig. 5a. The standard errors range from 0.11 s to 0.56 s for P waves and from 0.23 s to 0.70 s for S waves, several times larger than for ordinary earthquakes, probably because of the low frequency and complicated onsets of DLF earthquakes.

Relocated hypocenter distribution

The results of hypocenter relocations are shown in Fig. 5b. Colored hypocenter symbols correspond to the periods

from 1987 to 1994 (green), 1995 to August 2000 (blue) and September 2000 to May 2001 (red). The former two intervals correspond to ordinary activity before the DLF earthquake swarm, while the third interval includes the swarm activity of DLF earthquakes. Most DLF earthquakes form a cluster at the northeastern side of the summit, the center of which is located 3 km northeast of the summit. Approximately 90% of the selected DLF earthquakes are included in this main hypocenter zone, which has a horizontal dimension of about 5 km. The focal depths range from 11 to 20 km b.s.l.

There are seven earthquakes clearly located outside the main hypocenter region. Some of these are located on the southwestern side of the summit, while others are located on the southeastern side of the summit. As the nominal standard errors of the locations in this method are 2 to 3 km, the hypocenters outside the main zone are meaningful. In order to check the reliability of the arrival pick-up times, the original seismograms are examined for the event marked as A in Fig. 5b. Figure 6 compares the seismograms of A with those of B belonging to the main hypocenter region as shown in Fig. 5b. The arrival time differences between TRU and SSN are clear, indicating that the hypocenter of A is closer to SSN than B.

In the second step, the hypocenters of the 369 selected earthquakes in the period from 1995 to 2001 are determined by the ordinary hypocenter determination technique with the station corrections estimated in the first step. Figure 5c shows the resulting hypocenters of 344 events, with horizontal and vertical direction standard errors smaller than 1.5 km. The hypocenters of the two intervals, April 1995 to July 2000 and August 2000 to May 2001, are plotted in blue and red, respectively. The hypocenters of this dataset also
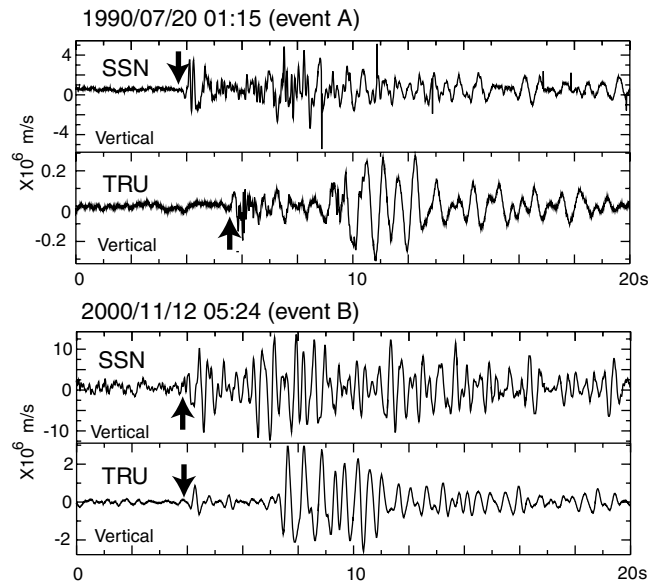

Fig. 6 Comparison of a pair of seismograms recorded at SSN and TRU for two DLF events. The *top graph* is an event at the southwestern side of the summit of Mount Fuji (event A in Fig. 5b), and the *bottom graph* is an event occurring in the main hypocenter region (event B in Fig. 5b)

Table 1 Standard seismic velocity structure

Depth (km below sea level)	Vp (km/s)	Vs (km/s)	Vp/Vs
0–2	4.0	2.3	1.74
2–4	5.0	2.9	1.72
4–12	6.0	3.6	1.67
12–29	6.7	3.85	1.74
29	7.8	4.45	1.75

show the same distribution pattern, forming an ellipsoidal cluster with a long axis oriented WNW–ESE (Fig. 5b). The center of the main cluster is located about 3 km from the summit to the NE. Apart from the main cluster, a sparse distribution around the summit of Mount Fuji can be seen in Fig. 5c. The focal depths of the 344 events range from 10 to 19 km.

Figure 5b and c indicate that most DLF earthquakes during the swarm period were concentrated within the main cluster region. A slight shift (2–3 km) of the epicenter region to the north can be distinguished at the time of the swarm activity in Fig. 5c. Nakamichi et al. (2004) reported that the hypocenters of the DLF earthquakes migrated 2–3 km from southeast to northwest during 1998–2001 on the basis of relocated DLF events by combining datasets of the NIED, Earthquake Research Institute of Tokyo University and Japan Meteorological Agency.

In order to examine effects of the standard seismic velocity structure on the hypocenter locations, hypocenters of 70 events are determined with station corrections by assuming velocity structures with low (-10%) velocities shallower than 12 km, and also with high velocities (5% at shallower than 4 km and 3% between 4 and 12 km). The resulting hypocenters for the 70 earthquakes are determined to be within 1 km, most of them within 0.5 km, for the epicenter and within 2 km for the focal depth compared to the standard velocity case.

Discussion

The occurrence rate and wave energy release of the DLF earthquakes indicate an abrupt initiation and cessation of swarm activity from October 2000 to May 2001. The swarm activity was likely caused by changes in and around the hypocenter zone. Tiltmeters installed at FJN, FJY, FJS and FJH stations, however, did not detect any abnormal tilt changes relating to magma migration to shallow depths (NIED 2002). At present, possible causes for DLF earthquake swarms are divided into two categories: magma movements and changes in tectonic setting. From the viewpoint of DLF earthquake swarm triggering, the commencement of the DLF earthquake swarm activity coincides with the cessation of magma migration in the Miyake-jima and Kozu-shima region, which was the most significant event in central Japan in 2000. In the same period, there were several unusual crustal events in central Japan. We first summarize them in order to determine the possible cause or causes of swarm activity.

The volcanic activity in the Miyake-jima and Kozu-shima region in 2000 consisted of two principal events: subsurface magma discharge at Miyake-jima (Ukawa et al. 2000; Geshi et al. 2002; Ueda et al. 2005) and dike intrusion between Miyake-jima and Kozu-shima during the same time (Nishimura et al. 2001). According to Nishimura et al. (2001) the total amount of magma discharged from Miyake-jima is estimated to be 0.7 km^3, while the amount of intruded magma between Miyake-jima and Kozu-shima is estimated to be 1.04 km^3. This activity presumably af-

fected both tectonic setting and the magma system around the intrusion area.

In order to examine volcanic and tectonic changes in the Mount Fuji area using the seismicity, four areas were selected as shown in Fig. 1; (a) the total area of Fig. 1, (b) the Mount Fuji area, (c) the Hakone area and (d) the eastern Yamanashi earthquake swarm area. The total area (a) represents the seismicity change of a relatively wide area including Mount Fuji. As the Mount Fuji area (b) and the Hakone area (c) are volcanic regions, their seismicity changes may reflect both magma activity and tectonic stresses in the surrounding regions. The eastern Yamanashi earthquake swarm region (d) exhibits fairly high seismicity even during normal periods, and therefore the stress state in this region is probably close to the critical state for fracturing. We thus expect that the seismicity in the eastern Yamanashi region is sensitive to changes of tectonic stress.

Figure 7 indicates the cumulative number of earthquakes in the four areas on the basis of the hypocenters by the Mount Fuji data processing system. Because of the improvement in the data processing system in January 2000, at which time we added several seismic stations of the Kanto-Tokai seismic network on the eastern side of Mount Fuji to the Mount Fuji dataset, the detection level is improved, especially for the eastern Yamanashi earthquake swarm region. As a result, the slope of the cumulative earthquakes changed in the eastern Yamanashi area at the beginning of 2000 (Fig. 7d). Owing to this effect the cumulative earthquake curve of the total area also exhibited a slight change in slope at the same time (Fig. 7a).

Regarding the DLF earthquake swarm for Mount Fuji, there is no significant change of occurrence rate for earthquakes in the total area (Fig. 7a) or in the eastern Yamanashi earthquake swarm area (Fig. 7d). On the other hand, in the Mount Fuji area a small step-like increase can be recognized during this period (Fig. 7b). This increase corresponds to the earthquake cluster near the FJY station at the southern slope of Mount Fuji as indicated in Fig. 1. The earthquakes in this cluster exhibit a tectonic type of strike slip mechanism with a P-axis in the N-S direction. In the Hakone area, a sharp increase of earthquakes is very clear in August 2001, immediately after the cessation of the DLF earthquake swarm in Mount Fuji (Fig. 7c). The high activity also reflects the occurrence rate for the total area in Fig. 7a. The crustal deformation observed by GPS and tiltmeters indicates dike-shaped inflation at shallow depths beneath Hakone volcano (Geographical Survey Institute 2002). The crustal deformation indicating dike intrusion is the first event to be recorded since the initiation of the GPS network and installation of tiltmeters in mid-1990s.

In 2002, several other dike intrusion events were observed in the eastern Izu (May 2002) and Hachijo-jima regions (August 2002). Figure 8 summarizes the locations of the active volcanoes and their active periods. The dike intrusion event at the eastern Izu peninsula (Ueda et al. 2003) is the first event after a four-year quiescence. The Hachijo-jima event is the first observation of high seismicity since the start of micro-earthquake observation by the NIED in

Fig. 7 Graph showing cumulative number of earthquakes not including DLF events and blasts in the regions indicated in Fig. 1. **a** Total area of Fig. 1, **b** Mount Fuji region, **c** the Hakone volcano region and **d** the earthquake swarm region of eastern Yamanashi. In **a**, the cumulative number of DLF events indicated in Fig. 4 is superposed with a *thick line*. The *shaded area* in each graph indicates the period of DLF earthquake swarm activity from October 2000 to May 2001
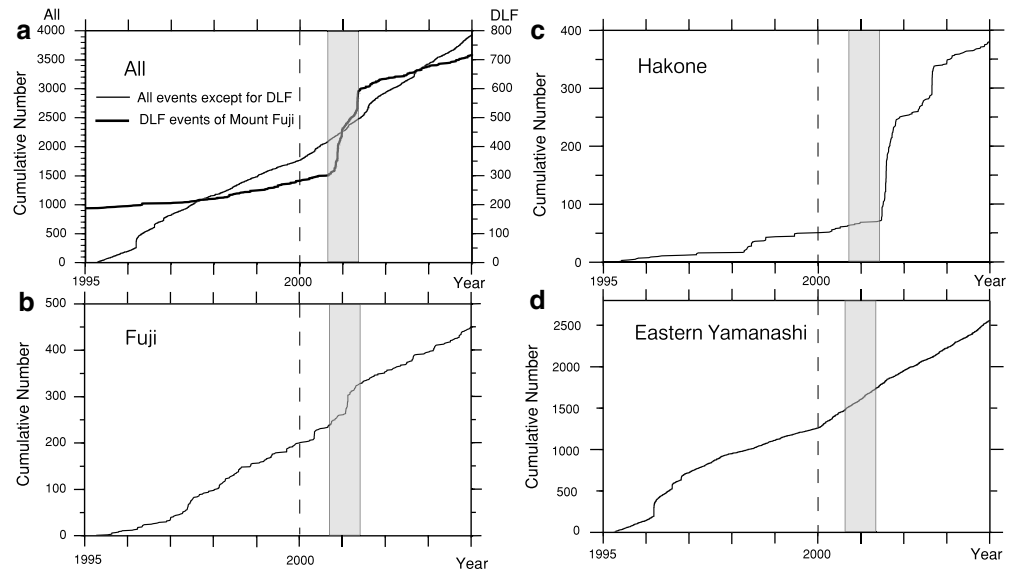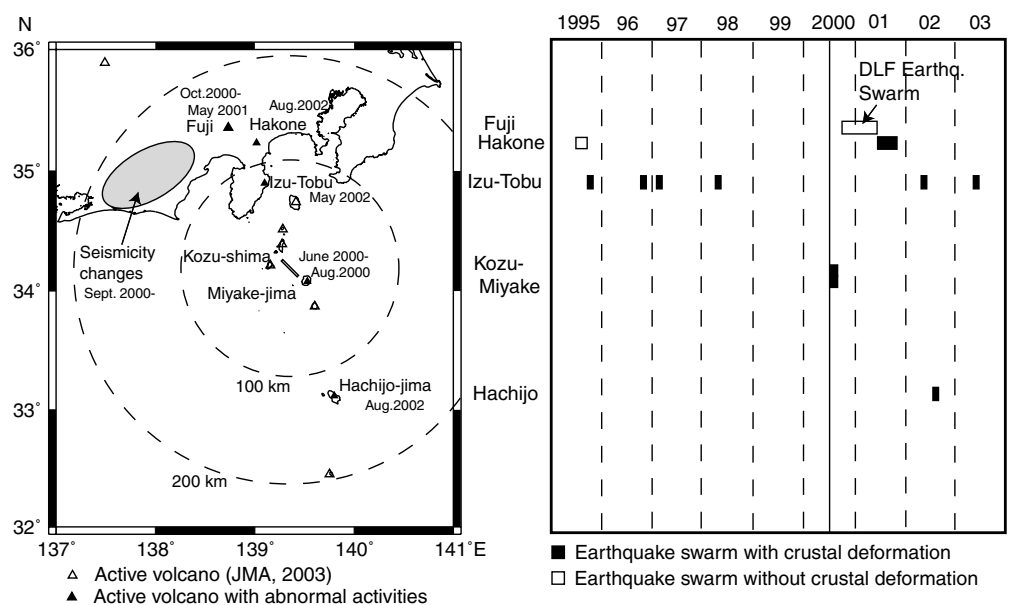
Fig. 8 (*Left*) Map showing tectonic and volcanic events since 2000. (*Right*) Chronological table showing the volcanic events around the Miyake-jima and Kozu-shima regions since 1995. The *vertical thin line* indicates the start of the 2000 Miyake-jima and Kozu-shima events

1983. Figure 8 suggests that magmatic activity along the Izu volcanic arc may have increased since the 2000 Kozu-shima and Miyake-jima events.

Slow slip and seismicity changes relating to the sub-duction of the Philippine Sea plate were reported (Ozawa et al. 2002; Matsumura 2003) in relation to crustal activity of the Tokai area (Fig. 8) on the western side of Mount Fuji. The GPS network of the Geographical Survey Institute, Japan, detected slow slip at the boundary of the subducting Philippine Sea plate around the western part of the Tokai district, which started soon after the volcanic activity in the Miyake-jima and Kozu-shima region. Matsumura (2003) observed seismicity changes in the subducting Philippine Sea plate and the overriding plate, which started in September 2000. The chronological coincidence among these three phenomena suggests the possibility that crustal activity in the Miyake-jima and Kozu-shima regions

affected the subduction of the Philippine Sea plate in the Tokai area, although the mechanism is not clear.

There is a close coincidence between dike intrusion in the Miyake-jima and Kozu-shima regions and the swarm activity of the DLF earthquakes at Mount Fuji, so we cal-culated static stress changes due to the dike intrusions. The magnitude of the stress change is on the order of 0.01 MPa around the Mount Fuji area, and the dominant compression is in the NNW-SSE direction. The static stress change is smaller than the stress drops of small earthquakes (0.1 to 1 MPa) (for example, Archuleta et al. 1982).

Summarizing the above, both tectonic and volcanic activity along the Izu volcanic arc has increased since the 2000 Kozu-shima and Miyake-jima dike intrusion event. The DLF earthquake swarm at Mount Fuji is considered to be one expression of this activity. Although no mechanism can be identified at present, the simultaneous activation

along the Izu volcanic arc suggests a connection to a deep magmatic system. The movements of magma at the Kozu-shima and Miyake-jima may have induced additional magma movements or pressure changes along the magma network in the crust or uppermost mantle.

Conclusions

On the basis of the DLF earthquake observations by the NIED seismic network, we investigated the temporal change of their occurrence rate from 1980 to 2003 and the hypocenter locations from 1987 to May 2001. The occurrence rate and the seismic wave energy release rate show an abrupt increase from October 2000 to May 2001, suggesting a change in the environment beneath Mount Fuji. Relocation of hypocenters of the DLF earthquakes indicates that hypocenters of the DLF earthquakes cluster mainly in an elongated region measuring 5 km along the long axis in a NW-SE direction, the center of which is located about 3 km NE from the summit. In addition to the main cluster, hypocenters extend to the southwest from the summit. During the swarm activity in 2000 to 2001, activity in the primary hypocenter region on the northeastern side of Mount Fuji increased greatly. The focal depths of well-located DLF events range from 10 to 20 km. The sharp increase of DLF earthquake activity at Mount Fuji began soon after magma discharge and intrusion events in the Miyake-jima and Kozu-shima region in July and August 2000. These events may have modified the state of the deep magmatic system beneath Mount Fuji, thus triggering the DLF earthquake swarm.

References

Aki k Richards PG (2002) Quantitative seismology, 2nd edn. University Science Books, Sausalito, CA, pp 1s– 700

Archuleta RJ, Cranswick E, Mueller C, Spudich P (1982) Source parameters of the 1980 Mammoth Lakes, California, earthquake sequence. J Geophys Res 87:4595–4607

Crosson RS (1978) Crustal structure modeling of earthquake data, 1.Simultaneous least squares estimation of hypocenter and velocity parameters. J Geophys Res 81:3036–3046

Hamada K, Ohtake M, Okada Y, Matsumura S, Sato H (1985) A high quality digital network for microearthquake and ground tilt observation in the Kanto-Tokai area, Japan. Earthqu Predic Res 3:447–469

Hasegawa A, Yamamoto A (1994) Deep, low-frequency microearthquakes in or around seismic low-velocity zones beneath active volcanoes in northeastern Japan. Tectonophysics 233:233–252

Hill DP (1996) Earthquakes and carbon dioxide beneath Mammoth Mountain, California. Seismolog Res Lett 67:8–13

Geshi N, Shimano T, Chiba T, Nakada S (2002) Caldera collapse during the 2000 eruption of Miyakejima Volcano, Japan. Bull Volcanol 64:55–68

Geographical Survey Institute (2002) Crustal deformation of Mt. Hakone and its surrounding area (in Japanese). Report on Coordinating Committee for Prediction of Volcanic Eruption 80:34–40

Koyama M (1998) Reevaluation of the eruptive history of Fuji volcano, Japan, mainly based on historical documents (in Japanese with English abstract). Bull Volcanol Soc Jpn 43:323–348

Koyanagi RY, Chouet B, Aki K (1987) Origin of volcanic tremor in Hawaii, Part 1, Data from the Hawaiian Volcano Observatory 1969–1985. Volcanism in Hawaii, US Geol Surv Prof Pap 1350:1221–1257

Matsumura S (2003) Spatio-temporal features of the seismicity occurring in the assumed locked area of the next Tokai earthquake (in Japanese with English abstract). Bull Earthqu Res Inst Univ Tokyo 78:269–282

Miyaji N (1988) History of younger Fuji volcano (in Japanese with English abstract). J Geol Soc Jpn 94:433–452

Miyaji N, Endo K, Togashi S, Uesugi Y (1992) Tephrochronological history of Mt. Fuji. 29th IUGG FIELD TRIP C12:75–109

Nakamichi H, Hamaguchi H, Tanaka S, Ueki S, Nishimura T, Hasegawa A (2003) Source mechanisms of deep and intermediate-depth low-frequency earthquakes beneath Iwate volcano, northeastern Japan. Geophys J Int 154:811–828

Nakamichi H, Ukawa M, Sakai S (2004) Precise hypocenter locations of midcrustal low-frequency earthquakes beneath Mt. Fuji, Japan. Earth Planet Space, 56:e37–e40

National Research Institute for Earth Science and Disaster Prevention (2002) Low-frequency earthquakes and tilt changes at Mount Fuji (in Japanese). Report on Coordinating Committee for Prediction of Volcanic Eruption 79:95–100

Nishimura T, Ozawa S, Murakami M, Sagiya T, Tada T, Kaidzu M, Ukawa M (2001) Crustal deformation caused by magma migration in the northern Izu Islands, Japan. Geophys Res Lett 28:3745–3748

Ozawa S, Murakami M, Kaidzu M, Tada T, Sagiya T, Hatanaka Y, Yarai H, Nishimura T (2002) Detection and monitoring of ongoing aseismic slip in the Tokai region, central Japan. Science 298:1009–1012

Sakai S, Yamada T, Ide S, Mochizuki M, Shiobara H, Urabe T, Hirata N, Shinohara M, Kanazawa T, Nishizawa A, Fujie G, Mikada H (2001) Magma migration from the point of view of seismic activity in the volcanism of Miyake-jima Island in 2000 (in Japanese with English abstract). J Geogr 110:145–155

Ueda H, Yamamoto E, Ohkubo T, Murakami M, Ueno H, Uhira K (2003) Tensile fault model of the crustal deformation associated with earthquake swarm in the eastern Izu Peninsula in May 2002 (in Japanese with English abstract). Bull Volcanol Soc Jpn 48:471–477

Ueda H, Fujita E, Ukawa M, Yamamoto E, Irwan I, Kimata F (2005) Magma intrusion and discharge process at the initial stage of the 2000 activity of Miyakejima, central Japan, inferred from tilt and GPS data (in press)

Ukawa M, Obara K (1994) Low-frequency earthquakes around Moho beneath the volcanic front in the Kanto district, central Japan (in Japanese with English abstract). Bull Volcanol Soc Jpn 38:187–197

Ukawa M, Ohtake M (1984) Peculiar microearthquake activity just beneath Mt. Fuji (in Japanese with English abstract). J Seismol Soc Jpn 37:129–133

Ukawa M, Ohtake M (1987) A monochromatic earthquake suggesting deep-seated magmatic activity beneath the Izu-Ooshima volcano, Japan. J Geophys Res 92:12649–12663

Ukawa M, Ishida M, Matsumura S, Kasahara K (1984) Hypocenter determination method of the Kanto-Tokai observation network for microearthquakes (in Japanese with English abstract). Res Note Natl Res Cent Disaster Prevent 53:1–88

Ukawa M, Eguchi T, Fuijnawa Y (1988) Seismic activity in the subducting Philippine Sea plate along the Suruga trough revealed by OBS observation. J Phys Earth 36:69–87

Ukawa M, Fujita E, Yamamoto E, Okada Y, Kikuchi M (2000) The 2000 Miyakejima eruption: Crustal deformation and earthquakes observed by the NIED Miyakejima observation network. Earth Planet Space, 52:xix–xxvi

White RA (1996) Precursory deep long-period earthquakes at Mount Pinatubo: spatio-temporal link to basaltic trigger. In: Newhall CG, Punongbayang RS (eds) Fire and mud: eruptions and lahars of Mount Pinatubo, Philippines. University of Washington Press, Seattle, Washington, pp 307–326